



Published in final edited form as:

*Curr Top Med Chem.* 2013 ; 13(4): 411–421.

## Gd-based macromolecules and nanoparticles as magnetic resonance contrast agents for molecular imaging

Ching-Hui Huang, Ph.D. and Andrew Tsourkas, Ph.D.\*

Department of Bioengineering, University of Pennsylvania, 240 Skirkanich Hall, 210 S. 33<sup>rd</sup> Street, Philadelphia, PA 19104

### Abstract

As we move towards an era of personalized medicine, molecular imaging contrast agents are likely to see an increasing presence in routine clinical practice. Magnetic resonance (MR) imaging has garnered particular interest as a platform for molecular imaging applications due its ability to monitor anatomical changes concomitant with physiologic and molecular changes. One promising new direction in the development of MR contrast agents involves the labeling and/or loading of nanoparticles with gadolinium (Gd). These nanoplatforms are capable of carrying large payloads of Gd, thus providing the requisite sensitivity to detect molecular signatures within disease pathologies. In this review, we discuss some of the progress that has recently been made in the development of Gd-based macromolecules and nanoparticles and outline some of the physical and chemical properties that will be important to incorporate into the next generation of contrast agents, including high Gd chelate stability, high “relaxivity per particle” and “relaxivity density”, and biodegradability.

### Keywords

contrast agent; gadolinium; macromolecule; magnetic resonance; molecular imaging; nanoparticle

## 1. Introduction

Magnetic resonance (MR) imaging contrast agents are widely used in medical diagnostic imaging due to their ability to improve tissue contrast and provide pathological correlates for a wide range of diseases. While various compounds have been evaluated as MR contrast agents, gadolinium (Gd) complexes continue to be the most widely used, and account for essentially all of the agents being used in the clinic today. Currently, all of the clinically-approved Gd complexes consist of individual Gd ions chelated with a low molecular weight acyclic or cyclic ligand (Figure 1). Due to their small size, many of these agents (e.g. Magnevist, Dotarem, DO3A) distribute throughout the intravascular and interstitial space and are rapidly cleared via renal filtration.

The pharmacokinetics and route of excretion of several Gd complexes have been altered by modifying the chemical properties of the Gd-chelate. For example, the presence of the lipophilic moiety on Multienhance (Gd-BOPTA) helps drive hepatic excretion, while a small ligand on Vasovist (MS-325, Ablavar) allows this complex to reversibly bind human albumin in plasma, leading to a plasma half-life of 2–3h[1]. This is markedly longer than Magnevist ( $t_{1/2}$  of only  $0.2 \pm 0.13$ hrs) (<http://berlex.bayerhealthcare.com/html/products/pi/>

\*To whom correspondence should be addressed. Dr. Andrew Tsourkas, 210 S. 33<sup>rd</sup> Street, 240 Skirkanich Hall, Philadelphia, PA 19104, Phone: 215-898-8167, Fax: 215-573-2071, [atsourk@seas.upenn.edu](mailto:atsourk@seas.upenn.edu).

Magnevist\_PI.pdf) and other clinical agents. Recent reports of other small molecules that can promote tissue or molecular-specific targeting[2] suggest that there is tremendous room for future developments in chelation chemistry; however, despite this promise, it is generally accepted that small Gd complexes cannot be used to differentiate between healthy and disease pathologies through binding of specific cell surface biomarkers. This is simply due to the inability of individual chelates to provide sufficient contrast via this targeting mechanism. For example, if it is estimated that a cancer cell has a volume of 1 pL (i.e. ~12.4 um diameter) and if it is assumed that each cancer cell has 1 million target receptors, the receptor concentration will only be 1.66 nM. Therefore, even if a tumor consisted entirely of cancer cells and all receptors were bound by Gd complexes, the concentration of Gd within the tumor would be ~5 orders of magnitude below the detection limit - the lower detection limit of most small Gd complexes (e.g. Magnevist) on a 1.5 T MR imaging system is considered to be ~100 μM[3]. Similarly, even if 10's of Gd complexes were attached to antibodies, to confer molecular specificity, and even if there was a 10-fold improvement in relaxivity owing to the slower rotational correlation time that results from attaching Gd to larger macromolecules[4], the signal amplification would still be ~3 orders of magnitude too low. This limitation has led to emerging interest in the development and use of Gd-based nanoparticles and macromolecules as MR molecular imaging contrast agents.

Numerous nanoparticles and macromolecules have already been explored as platforms for Gd-labeling and/or encapsulation, including polymers, proteins, dendrimers, micelles, and vesicles[5]. The value in preparing nanoparticles/macromolecules for molecular imaging applications stems from their ability to carry a large payload of Gd, the ease in which their physicochemical properties can be finely tuned, which can influence their pharmacokinetic and pharmacodynamic profiles, and the ability to readily functionalize their surface with molecularly specific targeting agents.

Despite their promise, early work with Gd-labeled macromolecules has revealed that translation of these agents to the clinic can be hampered by the slow, and in some cases, incomplete excretion of these larger agents[6–8]. Moreover, while Gd-complexes are generally considered safe when used in clinically recommended doses, there has been an expanding body of literature linking Gd to nephrotoxicity and Nephrogenic Systemic Fibrosis (NSF) in patients with kidney disease. It is hypothesized that prolonged tissue exposure to chelated Gd occurs in patients with reduced renal clearance, which may allow Gd to be released from its chelate and deposit in tissues. In response to concerns over NSF, it is now recommended that patients with acute kidney injury (AKI) and stage 4/5 chronic kidney disease (CKD) do not undergo Gd-enhanced MR imaging. The apparent relationship between poor Gd excretion and NSF is particularly concerning when developing Gd-based nanoparticles, because nanoparticles generally exhibit a much longer circulation and retention time in patients compared with small Gd complexes. Therefore, it is anticipated that in order to develop effective and safe Gd-based nanoparticles as MR contrast agents for molecule imaging, it will be necessary to strike a delicate balance between adequate circulation times for effective targeting and rapid excretion to minimize the likelihood of toxic side effects.

In this review, we will showcase Gd-based macromolecules and nanoparticles that have been developed for molecular imaging applications. Although a wide range of approaches will be discussed, particular emphasis will be placed on nanoparticles that exhibit a high relaxivity per nanoparticle, i.e. (relaxivity of Gd)×(Gd per nanoparticle), and a high “relaxivity density”, which we define as (relaxivity per nanoparticle)/(nanoparticle volume or molecular weight). To date, most Gd-based contrast agents are compared in terms of Gd relaxivity. While this parameter is important for perfusion and blood pool applications, where a higher relaxivity can mean a lower injected dose or higher contrast, it can be argued

that it is not an appropriate yardstick for molecular imaging contrast agents. For example, if a tumor cell has a fixed number of receptors on its surface, the binding of nanoparticles with 100,000 Gd/nanoparticle will certainly provide more contrast than binding of an individual Gd complex to each receptor, even if the Gd complex has a higher ion relaxivity. Moreover, since simply increasing the overall size of the nanoparticle will lead to a corresponding increase in the relaxivity per nanoparticle, in some instances it also makes sense to normalize to the nanoparticle volume or molecular weight to remove this potential bias and create a fair measure for comparison. A summary of the physical and magnetic properties of various macromolecule and nanoparticle-based MR contrast agents reported in this review are provided in Table 1.

In addition to providing an overview of various Gd-based nanoparticles, we will begin with a brief discussion on recent advances in the development of Gd ligands. Although individual chelated Gd complexes cannot be used for molecular imaging applications on their own, advances in this field are sure to benefit Gd-based nanoparticles since the relaxivity of individual Gd complexes directly contribute to the overall relaxivity per nanoparticle and relaxivity density.

## 2. Gadolinium chelates

As noted above, a number of gadolinium chelates have been approved for clinical applications (Figure 1), all of which can be classified as either cyclic or acyclic. The macrocyclic ligands, e.g. DOTA and DO3A, are derivatives of 1,4,7,10-tetraazacyclododecane (cyclen) and the acyclic ligands, e.g. DTPA and DTPA-BMA, are derivatives of polyaminocarboxylic acids. Cyclic ligands are more stable in comparison to acyclic ligands, with  $[\text{Gd}(\text{DOTA})]^{-1}$  exhibiting an in vitro stability that is five orders of magnitude higher than  $[\text{Gd}(\text{DTPA})]^{-2}$  and an exceedingly slow metal ion dissociation even at very low pH[9]. Therefore, it is no surprise that NSF has almost exclusively been linked to linear Gd chelates. For example, while over 8 million patients have been injected with the cyclic compound Gd-HP-DO3A/gadoteridol/Prohance® (<http://usa.braccoimaging.com/prohance/prohance.html>), there is only one reported case of NSF associated with gadoteridol use alone[10, 11]. Further, there are no reported cases of NSF in patients that received Gd-DOTA/gadoterate/Dotarem®[10]. Therefore, from a safety perspective, DOTA is certainly the recommended choice for use in Gd-based nanoparticles.

To allow for lower injected doses of Gd and/or improve Gd-mediated contrast, numerous groups have been working towards developing Gd ligands with improved relaxivity (Figure 2). The predominant approach involves synthesizing ligands that allow a higher number of water molecules to coordinate with Gd. For example, Raymond et.al. published a new class of ligands based on hexadentate hydroxypyridinone (HOPO), which almost doubles the relaxivity compared with DTPA and DOTA, due to its ability to coordinate a second inner sphere water molecule[12]. Similarly, Aime et. al. developed a polyaminocarboxylate based contrast agent  $[\text{Gd}(\text{AAZTA})]^{-1}$ , which also permits more than one inner-sphere water, resulting in a relaxivity value of  $7.1 \text{ mM}^{-1}\text{s}^{-1}$  at 20 MHz and 25 °C[13]. However, in both cases the reduction in the number of donor atoms in the chelating ligands decreases the thermodynamic and kinetic stability of the chelates[14] thus raising concerns over toxicity in clinical applications.

In an alternative approach, the relaxivity of chelated Gd has also been improved by increasing the water exchange rate. This has been achieved by introducing steric constraints on the water-binding site. In the complex  $[\text{Gd}(\text{EGTA})]^{-1}$  (EGTA=3,12-bis(carboxymethyl)-6,9-dioxa-3,12-diazatetradecanedioate), the ethyl group bridging the two coordinating oxygens causes a steric compression around the water binding site[15, 16].

This destabilizes the metal bound water molecule, thus resulting in an accelerated exchange rate. The  $[\text{Gd}(\text{EGTA})]^{-1}$  derived contrast agent showed an enhanced relaxivity of  $7.0 \text{ mM}^{-1}\text{s}^{-1}$  at 20 MHz and  $25^\circ\text{C}$ [15]. Although  $[\text{Gd}(\text{EGTA})]^{-1}$  demonstrated much higher relaxivity than commercially available contrast agents, EGTA suffers from poor thermodynamic stability. More recent studies have suggested that stability can be improved through the replacement of carboxylate groups with phosphonates or by introducing aromatic moieties into the oxoethylene bridge[17, 18]. These modifications also enable the possibility of nanoparticle conjugation.

A new complexation method that leads to a dramatic improvement in Gd relaxivity over current commercial chelates involves entrapping Gd in a fullerene, i.e. buckyball. The first metallofullerene was designated as  $\text{Gd}@C_{82}$ , with @ indicating the incorporation of  $\text{Gd}^{3+}$  in the interior of the fullerene[19]. To increase the water solubility, Mikawa et. al. modified the exterior of the fullerene with the hydroxyl groups to produce  $\text{Gd}@C_{82}(\text{OH})_n$  (Gd-fullerenols). Elementary chemical analysis indicated that fulleranol has 30–40 hydroxyl groups and 11–15 coordinated water molecules via hydrogen bonds[20], and  $\text{Gd}@C_{82}(\text{OH})_{40}$  demonstrated a 20-fold higher relaxivity than that of Gd-DTPA at 1T[21] ( $r_1 = 67 \text{ mM}^{-1}\text{s}^{-1}$  at 0.47T,  $25^\circ\text{C}$ ). Interestingly, this high relaxivity was not produced by direct interaction between the bulk water molecules and the gadolinium ion. Electron energy loss spectroscopy (EELS) results indicated the high relaxivity was caused by the paramagnetic electronic structure of the metallofullerene as a result of a 3-electron transfer from gadolinium to the fullerene cage[20, 22]. Thus, the hydrogen bond protons of the water molecules on the metallofullerene surface undergo relaxation. Gd-metallofullerene is expected to possess a high biological safety in regards to Gd-mediated toxicity, since Gd ions are entrapped within a stable carbon cage. Several recent studies have also shown that cells can be labeled with  $\text{Gd}@C_{60}[\text{C}(\text{COOH})_2]_{10}$  with no major adverse effects reported, making them an interesting candidate for molecule imaging studies[23, 24].

### 3. Macromolecular Contrast Agents

#### 3.1 Linear Polymeric Macromolecules

Early macromolecular contrast agents utilized linear natural or synthetic polymers, i.e., protein human serum albumin, HSA), polyamino acids (poly(L-lysine)), or oligosaccharides (dextran) as platforms for Gd labeling (Figure 3). The primary advantages of using proteins include their homogeneity and their availability/abundance. The primary disadvantage for molecular imaging applications is their limited capacity for labeling with Gd, e.g., HSA contains 57 lysines and a typical synthesis yields only 20 to 35 molecules of Gd per albumin. In addition, the use of foreign proteins can elicit an immunogenic response[8, 25]. Consequently, linear synthetic polyamino acids, such as Gd-DTPA polylysine[26–28], polyglutamic acid[29], and poly(N-hydroxypropyl-L-glutamine)[30] have generally garnered more attention as macromolecular MR contrast agents. For comparison, polylysine of the same molecular weight as HSA has more than 500 lysine residues that are accessible for conjugation and even higher molecular weight chains are available (>400 kDa) if higher Gd payloads are required. The large capacity for Gd labeling per macromolecule makes polyamino acids very attractive for MR molecular imaging applications. Attachment to polyamino acids also prolongs the blood circulation time[28] and increases the relaxivity of Gd due to a slower rotational correlation time. For example, polylysine with a molecular weight of 480kDa has a blood half life of 429 minutes[28] and the attached Gd has a relaxivity of  $10.8 \text{ mM}^{-1}\text{s}^{-1}$  (0.4T at  $39^\circ\text{C}$ )[31]. Recently, it has been shown the folate-conjugated, Gd-labeled polylysine can be used to specifically detect folate receptor expression in murine tumor xenografts[32]. Notably, the plasma half-life of polylysine can be extended through the addition of MPEG (i.e. grafted co-polymer); however, animal studies revealed that these compounds exhibit incomplete excretion after 12 days[7].

Similar to polyamino acids, polysaccharides also provide an intriguing linear platform for carrying high Gd payloads[33, 34]. Dextran is a water soluble and biodegradable polysaccharide that has been used medicinally as an antithrombotic and volume expander in anemia[35]. It has been shown that a 165kDa dextran can be labeled with as many as 187 Gd per molecule. In a separate study, it was shown that the relaxivity of Gd following conjugation to dextran (75 kDa) was  $10.5 \text{ mM}^{-1}\text{s}^{-1}$  (0.25T, 37°C)[36]. Therefore, it can be roughly approximated that the resulting relaxivity density can be at least  $\sim 26.18 \text{ mM}^{-1}\text{s}^{-1}/\text{kDa}$ [34]. Unfortunately, dextran does suffer from a high degree of polydispersity, which makes it difficult to repeatedly prepare identical formulations. Moreover, anaphylactic reactions have been noted for higher molecule weight dextrans[37, 38]. Other polysaccharides that have also been evaluated as MR contrast agents include inulin, hydroxyethyl starch, and chitosan oligosaccharides[39–41].

Another synthetic approach that has been used to create macromolecules with high Gd payloads, involves the direct tethering of Gd chelates, i.e. cascade polymers[42], or the formation of linear copolymers whereby PEG, polypropylene glycol (PPG)[43], or cystine linkers[44, 45] are placed between monomeric chelate units (Figure 3). These compounds have typically been synthesized with molecular weights below 50 kDa; however, larger constructs could be created for molecular imaging applications if so desired, although this will likely come at the cost of increased polydispersity. In general, the relaxivity density of cascade co-polymers can be fairly high, considering the low amount of extraneous materials used in the preparation. For example, cascade-Gd-DTPA-24 ( $\sim 30\text{kDa}$ ) is composed of 24 Gd chelates and the relaxivity per Gd is  $10 \text{ mM}^{-1}\text{s}^{-1}$  (2T, 37°C)[42, 46]. Therefore, the relaxivity per macromolecule is  $240 \text{ mM}^{-1}\text{s}^{-1}$  and the relaxivity density is  $8 \text{ mM}^{-1}\text{s}^{-1}/\text{kDa}$ . Since some current formulations can only be functionalized with targeting ligands at the termini, additional chelation chemistry may be required to allow for higher labeling with targeting agents. Nonetheless, linear co-polymer chains do provide an interesting direction for future research.

One particularly valuable characteristic for most of the linear macromolecules discussed in this section is their ability to be degraded into smaller units and cleared. For example, it has been shown that lysosomal enzymes (e.g. cathepsin B) can degrade poly(L-glutamic acid) back to individual units of L-glutamic acid[29]. Similarly, it has been shown that Gd-labeled polydisulfide-based co-polymers (cystine linkers) are slowly reduced in circulation[42, 44, 45, 47–51], while still generating significant contrast enhancement in the blood pool for as long as  $\sim 0.5$  hours.

### 3.2 Dendrimers and Dendrimer Nanoclusters

Dendrimers have become a popular platform for constructing multifunctional agents for therapeutic and diagnostic purpose due to their defined structure, the ability to tightly control dendrimer size and the presence of multivalent surface groups[52]. The high density of surface groups is particularly appealing for the development of highly paramagnetic Gd-based contrast agents for molecular imaging (Figure 4). For example, a generation 10 PAMAM dendrimer has a total of 4096 amines that are available for possible conjugation with Gd chelates. In one report, generation 10 dendrimers were labeled with 1860 Gd, with each Gd possessing a relaxivity of  $36 \text{ mM}^{-1}\text{s}^{-1}$ [53]. Therefore, the relaxivity per nanoparticle was  $66,960 \text{ mM}^{-1}\text{s}^{-1}$  and the relaxivity density was  $22.3 \text{ mM}^{-1}\text{s}^{-1}/\text{kDa}$ .

Recently, a new approach for the preparation of bifunctional DOTA and DTPA chelates was reported, which further enhanced the relaxivity of Gd-labeled dendrimers and reduced the possibility of free Gd ions from becoming entrapped within the dendrimer core during the chelation process. This method pre-complexed the gadolinium chelates in alcohol prior to conjugation to dendrimers (pre-metalation), thus the free metal ions could easily be removed



prior to dendrimer labeling. In comparison to the analogous G4 dendrimer-based agent prepared by the post-metalation method, the agent prepared via the pre-metalation method demonstrated a higher Gd relaxivity value ( $r_1 = 26.9$  vs  $13.9 \text{ mM}^{-1}\text{s}^{-1}$  at 3T and 22 °C)[54, 55].

While generation 10 dendrimers have not yet been tested as targeted MR contrast agents, generation 4 and 5 PAMAM dendrimers (64 and 128 surface amines, respectively) have previously been used to image folate receptor expression in tumor xenografts[56, 57]. Although generation 5 dendrimers typically possess a total relaxation per nanoparticle (Table 1) that is below the expected threshold for molecular imaging, it is hypothesized that these targeted contrast agents may have benefited from receptor-mediated internalization and recycling, thus providing a natural signal amplification mechanism, i.e. the same receptor can continually internalize new dendrimers[57].

It is reasonable to assume that improved tumor contrast could have been achieved if higher generation dendrimers were utilized in the above studies; however, high generation dendrimers (>10) are often difficult to prepare owing to the many protection/deprotection steps and the lowering yields associated with each new generation. The solubility of high generation dendrimers can also be problematic. These shortcomings have recently led to the development of dendrimer nanoclusters (DNCs)[58]. DNCs are composed of individual gadolinium-labeled PAMAM dendrimers that are crossed-linked to form large nanoparticles (Figure 4). This design allows for the use of low generation dendrimers, which are easier to synthesize and solubilize, but also benefits from a large number of surface groups for Gd labeling, which are only available with larger nanoparticles. The overall DNC size and porosity can also be adjusted by altering the synthetic conditions and linker length, respectively, to ensure high water permeability[58]. Because of their larger size, DNCs exhibit a higher  $r_1$  value per gadolinium in comparison to individual gadolinium-labeled PAMAM dendrimers ( $12.3$  vs.  $10.1 \text{ mM}^{-1}\text{s}^{-1}$  for generation 5 dendrimers). Further, it has been shown that a 150 nm DNC can be labeled with ~300,000 gadoliniums. Therefore, on a per particle basis the  $r_1 = 3.6 \times 10^6 \text{ mM}^{-1}\text{s}^{-1}$  at 1.41T and 40°C. Due to their high relaxivity, DNCs functionalized with folic acid were capable of specifically detecting folate receptor-positive tumors in mouse xenografts. More recently, it has been shown that biodegradable polydisulfide DNCs can also be formed, through the use of PEG-disulfide linkers[59]. These agents exhibited a serum half-life of 1.6 hrs and low tissue retention at 24 hours. Therefore, these agents present an exciting direction for future molecular imaging applications.

### 3.3 Liposomes and Polymersomes

Liposomes have been transformed into paramagnetic contrast agents by either encapsulating chelated Gd within the aqueous lumen or by immobilizing the chelated Gd on the membrane surface. Although, liposomes with encapsulated Gd-chelates have previously been used for contrast-enhanced MR imaging, the slow flux of water across the membrane bilayer does impair the water exchange rate with encapsulated Gd and thus leads to a significant reduction in relaxivity[60]. This can be partially overcome by increasing the surface-to-volume ratio (i.e., decreasing the size of the vesicle); however, even liposomes that are 100 nm in diameter exhibit a relaxivity (per Gd) that is 62% lower than free chelated Gd[60, 61]. Cholesterol, which is generally required to increase the stability of liposomes, further reduces the relaxivity of encapsulated Gd[62]. Therefore, the immobilization of chelated Gd on the surface of the bilayer membrane has become the preferred embodiment for vesicle-based MR agents, since surface-bound Gd has much better water accessibility than encapsulated Gd. Further, an additional advantage of attaching chelated Gd to the nanovesicle surface is the enhancement in the  $r_1$  per Gd[63], which has been attributed to the slowed rotational correlation time, compared with free chelated Gd in solution.

The idea of developing nanovesicles with encapsulated Gd was recently revisited with the development of paramagnetic porous polymersomes (Figure 4). The foreseen advantage of loading chelated Gd within the intravesicular volume was that much higher Gd payloads could be obtained, and thus higher relaxivities per particle - if improved water permeability could be achieved[64]. Compared to liposomes, polymersomes possess several beneficial properties, including increased mechanical stability[65, 66] and the ability to be finely tuned through polymer selection, to yield vesicles with diverse functionality, i.e biodegradability, biocompatibility, elasticity, etc. However, most polymersomes are significantly less permeable to water than liposomes[65]. Therefore, membrane permeability was achieved by introducing pores into the vesicle bilayer[67, 68]. Two different approaches have been taken to create porous polymersomes. In the first approach, polymersomes were produced from the aqueous assembly of polyethylene oxide-*b*-polybutadiene, PEO-PBD, in the presence of a small percentage of phospholipids. The polymers were crosslinked using a chemical initiator and the phospholipids was extracted with surfactant, generating a highly porous outer membrane[68]. In a second approach, the porous polymersomes were produced through the aqueous assembly of two polymers, PEO-PBD and the hydrolytically-labile diblock copolymer, polyethylene oxide-*b*-polycaprolactone (PEO-PCL)[67]. Subsequent acid hydrolysis of the caprolactone block resulted in a permeable outer membrane. For both porous vesicles, paramagnetic agents were produced by encapsulating chelated-Gd. To prevent the small Gd-chelates from leaking through the porous membrane, Gd-chelates were attached to dendrimers prior to their encapsulation. It was found that the porous polymersomes, 130 nm in diameter, had an  $r_1$  relaxivity value of  $7.5 \text{ mM}^{-1}\text{s}^{-1}$  per Gd. For comparison, non-porous vesicles with Gd-DTPA encapsulated within the lumen had an  $r_1$  of  $1.7 \text{ mM}^{-1}\text{s}^{-1}$  per Gd. Further, it was estimated that there were  $\sim 40,000$  Gd per polymersome. Therefore, the resultant relaxivity ( $r_1$ ) per porous polymersome was calculated to be  $\sim 3 \times 10^5 \text{ mM}^{-1}\text{s}^{-1}$ .

The pharmacokinetics of the paramagnetic porous polymersomes revealed a circulation half-life of  $> 3.5$  h, which is considerably shorter than the half-life of analogous polymersomes[69] ( $t_{1/2} > 15\text{h}$ ). Further, biodistribution and MR-enhancement studies indicated that the porous polymersomes were gradually destabilized in circulation and excreted via renal filtration.

### 3.4 Micelles and Nanoemulsions

One interesting approach that has recently been taken to create high relaxivity macromolecular contrast agents involves developing Gd-labeled amphiphilic compounds that can self-aggregate into micellar nanoparticles[70]. The hydrophobic blocks are orientated toward the core of the particles, while the hydrophilic moieties (i.e. Gd-chelates) are exposed to the solvent. Micelles formed in this manner exhibited a relaxivity of  $18.01 \text{ mM}^{-1}\text{s}^{-1}$  on a per ion basis (20MHz, 25°C). A 10% increase in relaxivity was observed following the incorporation of cholesterol into the hydrophobic interior, due to the increased rigidity and reduced rotational flexibility of the chelated Gd.

A higher relaxivity of  $22.6 \text{ mM}^{-1}\text{s}^{-1}$  and  $24.2 \text{ mM}^{-1}\text{s}^{-1}$  (at 20MHz and 25°C) was achieved when amphiphilic Gd-chelates were derived from DTPA and DOTA[71, 72]. Botta et. al. reported the synthesis of a Gd-DOTA derivative functionalized with two hydrophobic chains on adjacent pendant arms [Gd-(DOTA(GAC)<sub>12</sub>)<sub>2</sub>][73]. This compound exhibited remarkable relaxivity values when embedded into micelles ( $r_1 = 34.8 \text{ mM}^{-1}\text{s}^{-1}$ , at 20MHz and 25°C), since the presence of two aliphatic chains on adjacent acetic arms greatly reduced the fast rotation of the Gd-chelates.

Highly paramagnetic micelles have also been created through post labeling of pre-formed micelles. For example, 38 nm micelles formed from the diblock copolymer poly(acrylic

acid)-b-poly(methyl acrylate), also known as shell-crosslinked knedel-like (SCK) nanoparticles, were labeled with 510 Gd atoms (Figure 4). The Gd relaxivity in these formulations was  $39 \text{ mM}^{-1}\text{s}^{-1}$  (0.47 T and 40°C) and the relaxivity on a per particle basis was  $19,890 \text{ mM}^{-1}\text{s}^{-1}$ [74].

Perfluorocarbon (PFC) nanoemulsions represent another promising platform whereby amphiphilic compounds were labeled with Gd (Figure 4); in this case Gd-labeled phospholipids were used to stabilize PFC emulsions in an aqueous environment. The presence of Gd on the outer surface of the nanoemulsion and PFC within the core[75, 76], allowed these agents to be used for both  $T_1$ - and fluorine-imaging. The first generation of paramagnetic PFC nanoemulsions (250 nm) utilized the amphiphile, Gd-DTPA-BOA (gadolinium-diethylenetriamine-pentaacetic acid bis-oleate), and carried Gd payloads of up to 100,000 per particle[75]. Substitution of the twin oleic acids with a naturally occurring membrane phospholipids (phosphatidylethanolamine, PE) to anchor the Gd chelated to the outer lipid monolayer enhanced the Gd relaxivity from  $17.7 \text{ mM}^{-1}\text{s}^{-1}$  to  $33.7 \text{ mM}^{-1}\text{s}^{-1}$  (1.5T at 37 °C)[77]. To reduce any potential toxicity, gadolinium-methoxy-DOTA-PE based nanoparticles were also developed. These macrocyclic DOTA-based PFC nanoemulsions diminished the transmetalation of gadolinium in the presence of  $\text{ZnCl}_2$  in comparison to the acrylic DTPA-based particles[78]. Following these improvements, PFCs have been reported to possess relaxivities as high as  $2.48 \times 10^6 \text{ mM}^{-1}\text{s}^{-1}$  on a per particle basis. This high relaxivity has allowed these agents to be used for a variety of molecular imaging applications, including the imaging of tumors, atherosclerotic plaques, and restenosis[79–81].

### 3.5 Silica Nanoparticles

Mesoporous silica nanoparticles (MSNs) represent another interesting nanopatform for Gd labeling due to their uniform mesopores, biocompatibility and functionality[82, 83]. The large surface area that results from the highly porous structure allows for the loading of high Gd payloads. Silica nanoparticles with different sizes and shapes have been reported as contrast agents. For example, the mesoporous silica SBA-15 has been used to create rod-like particles (600–700 nm) with 80 Å pores[84], while MCM-41 has been used to create spherical nanoparticles (20–50 nm) with 35 Å pores. Interestingly, despite their smaller pores, MCM-41 MSNs actually demonstrated a higher relaxivity ( $r_1=27 \pm 2 \text{ mM}^{-1}\text{s}^{-1}$ , at 20 MHz and 37°C) than SBA-15 MSNs ( $6.7 \pm 0.3 \text{ mM}^{-1}\text{s}^{-1}$ ), after conjugation with Gd-DOTAMA. It was hypothesized that these findings stem from the localization of the Gd-complex on the inner or outer surface of the MSN, which is largely dictated by the pore size.

### 3.6 Gd Oxide Nanoparticles and Gd-loaded nanotubes

Recently, there has been increasing interest in the use of magnetic inorganic particles, e.g.  $\text{Gd}_2\text{O}_3$  and Gd-loaded nanotubes, as MRI contrast agents. Small nanoparticle  $\text{Gd}_2\text{O}_3$  (SPGO), with diameters between 20 and 40 nm, were found to possess Gd relaxivities comparable to Gd-DTPA chelates[85]. Ultrasmall nanoparticle  $\text{Gd}_2\text{O}_3$  (USPGO), with diameters between 3 to 10 nm, exhibited twice the relaxivity compared to Gd-DTPA[86]. Considering the tight packing of Gd within  $\text{Gd}_2\text{O}_3$  nanoparticles (200 Gd per 3 nm particle[87]), these nanoparticles present an interesting research direction; however, concerns over the release of free  $\text{Gd}^{3+}$  ions may inhibit their clinical utility. Recent efforts focused on coating  $\text{Gd}_2\text{O}_3$  with various materials, in order to reduce the potential toxicity, presents a possible solution, but the presence of non-chelated Gd does remain worrisome[88].

Similar concerns limit the translatability of Gd-loaded nanotubes, but their interesting magnetic properties do warrant at least a brief discussion. Gd-loaded nanotubes are



constructed by chemically cutting single-wall carbon nanotubes (SWNTs) into ultra-short nanotubes (20–100nm, US-tubes)[89]. The exterior of the US-tubes provide a versatile scaffold for the conjugation of targeting ligands, while the interior space is used to encapsulate Gd ions. The first carbon nanotube-based contrast agent called “gadonanotube” was reported by Sitharaman et. al. (Figure 4)[90]. These  $Gd^{3+}_n@US\text{-tubes}$  are linear molecular magnets with Gd ion relaxivities as high as  $180\text{ mM}^{-1}\text{s}^{-1}$  (60 MHz, 40 °C). This high relaxivity is due to the formation of small clusters of 3 to 10 Gd within sidewall defects, which exhibit superparamagnetic properties. Each nanotube contains approximately 100 Gd ions[91]. Surface modification and functionalization with various amino acids and peptides have promoted the development of gadonanotubes as targeted MR contrast agents[92]; however, as noted above, the release of non-chelated Gd into circulation remains a potential concern.

### 3.7 Natural biological nanoparticles

Virus-like particles (VLPs) are a special class of multimeric proteins that form protein shells with an empty interior space. These highly ordered and nanoscale protein building blocks make VLPs an interesting platform for developing multifunctional agents owing to their highly uniform core-shell structure and the high density of chemically reactive groups on the outer surface. VLPs derived from the coat of the bacteriophage were functionalized with chelated Gd and poly(ethylene glycol) (PEG) units. VLPs composed of MS2 capsids were labeled with as many as 515 Gd, with each Gd exhibiting a relaxivity of  $14\text{ mM}^{-1}\text{s}^{-1}$ . The relaxivity per VLP was  $7200\text{ mM}^{-1}\text{s}^{-1}$  (1.5 T)[93, 94]. Notably, the polymer assembly on each VLP does not significantly restrict water exchange between the bulk water and VLP interior, as was seen in some polymersomes and liposomes, which makes Gd encapsulation a viable approach.

Recently, bacteriophage P22-based VLPs were modified with the primary amine rich polymer, AEMA, to further increase the number of functional groups on the VLP surface.  $P22_{s39c}\text{-xAEMA-Gd}$  nanoparticles exhibited a relaxivity of  $22.0\text{ mM}^{-1}\text{s}^{-1}$  (1.4T) per Gd ion. Further, the ability to functionalize each VLP with  $9,100\pm 800$  Gd led to an  $r_1$  of  $200,000\text{ mM}^{-1}\text{s}^{-1}$  per  $P22_{s39c}\text{-xAEMA-Gd}$  nanoparticle, which surpasses the previously reported VLPs[95, 96].

Similar to VLPs, lipoproteins are natural biological nanoparticles that have been used as a nanoplatform for Gd-labeling. Lipoproteins are composed of a phospholipid monolayer encapsulating a hydrophobic core. Both high-density lipoproteins (HDLs) and low-density lipoproteins (LDLs) have been extensively studied as nanoplatforms owing to their important physiological functions. For example, due to the nature of HDL to transport cholesterol from the peripheral tissue to the liver, HDL nanoparticles have been developed to target hepatocytes and atherosclerotic plaques[97]. LDL nanoparticles have been developed as MRI contrast agents for malignant cells expressing LDL receptors[98]. Amphiphilic gadolinium-DPTA chelates have been incorporated into lipoproteins to produce lipoprotein-like nanoparticles. Zheng et. al. reported that 150 to 496 Gd could be incorporated into each LDL nanoparticle[99]. For an LDL nanoparticle containing 180 amphiphilic Gd chelates, the  $r_1$  per Gd was  $7.9\pm 0.22\text{ mM}^{-1}\text{s}^{-1}$  at 60 MHz - thus the  $r_1$  per LDL particle was estimated to be  $1440\text{ mM}^{-1}\text{s}^{-1}$ . In vitro studies showed that LDL-like Gd nanoparticles retained a similar hydrodynamic size and surface charge as the natural LDL particle and retained selective cellular binding and uptake. The design of this biocompatible nanoplatform greatly expands the possible application of lipoprotein nanoparticles in diagnostic imaging.

## 4. Conclusion and future outlook

Currently, all clinically-used Gd-based contrast agents are monomeric Gd(III) chelates; however, over the last decade, Gd-based nanoparticles and macromolecules have garnered a high degree of interest as molecular imaging agents due to their ability to carry high Gd payloads and their versatile composition. However, when designing nanoparticles for imaging applications, one must keep in mind the chemical and biological limits for MR imaging. Attempts to maximize the gadolinium payload and increase the rotational correlation time by increasing molecular weight are often compromised by low water solubility, lack of scalability, poor pharmacokinetics, and protracted elimination. Although great progress has been made in overcoming these hurdles, many challenges still remain before Gd-based nanoparticles can become a viable option for clinical use. As we continue to move towards an approach of “personalized medicine”, molecular imaging will undoubtedly become a vital part of routine patient management and Gd-based nanoparticles offer an exciting opportunity to fill this need.

## Acknowledgments

This work was supported in part by the National Institute of Health (NIH) NIBIB/R01-EB012065, NCI/R01-CA157766, and NIBIB/R21-EB013226.

## References

1. Parmelee DJ, Walovitch RC, Ouellet HS, Lauffer RB. Preclinical Evaluation of the Pharmacokinetics, Biodistribution, and Elimination of MS-325, a Blood Pool Agent for Magnetic Resonance Imaging. *Invest. Radiol.* 1997; 32:741–747. [PubMed: 9406014]
2. Weissleder R, Kelly K, Sun EY, Shtatland T, Josephson L. Cell-specific targeting of nanoparticles by multivalent attachment of small molecules. *Nat. Biotechnol.* 2005; 23(11):1418–1423. [PubMed: 16244656]
3. Caravan P. Strategies for increasing the sensitivity of gadolinium based MRI contrast agents. *Chem. Soc. Rev.* 2006; 35(6):512–523. [PubMed: 16729145]
4. Botta M, Tei L. Relaxivity Enhancement in Macromolecular and Nanosized GdIII-Based MRI Contrast Agents. *Eur. J. Inorg. Chem.* 2012; 12:1945–1960.
5. Louie A. Multimodality Imaging Probes: Design and Challenges. *Chem. Rev.* 2010; 110(5):3146–3195. [PubMed: 20225900]
6. Barrett T, Kobayashi H, Brechbiel M, Choyke PL. Macromolecular MRI contrast agents for imaging tumor angiogenesis. *Eur. J. Radiol.* 2006; 60(3):353–366. [PubMed: 16930905]
7. Bogdanov AA Jr, Weissleder R, Frank HW, Bogdanova AV, Nossif N, Schaffer BK, Tsai E, Papisov MI, Brady TJ. A new macromolecule as a contrast agent for MR angiography: preparation, properties, and animal studies. *Radiology.* 1993; 187(3):701–706. [PubMed: 8497616]
8. Brasch RC. Rationale and applications for macromolecular Gd-based contrast agents. *Magn. Reson. Med.* 1991; 22(2):282–287. discussion 300-283. [PubMed: 1725917]
9. Bousquet JC, Saini S, Stark DD, Hahn PF, Nigam M, Wittenberg J, Ferrucci JT. Gd-DOTA: characterization of a new paramagnetic complex. *Radiology.* 1988; 166(3):693–698. [PubMed: 3340763]
10. Penfield JG, Reilly RF. Nephrogenic systemic fibrosis risk: is there a difference between gadolinium-based contrast agents? *Semin. Dial.* 2008; 21(2):129–134. [PubMed: 18225999]
11. Reilly RF. Risk for nephrogenic systemic fibrosis with gadoteridol (ProHance) in patients who are on long-term hemodialysis. *Clin. J. Am. Soc. Nephrol.* 2008; 3(3):747–751. [PubMed: 18287249]
12. Werner EJ, Avedano S, Botta M, Hay BP, Moore EG, Aime S, Raymond KN. Highly Soluble Tris-hydroxypyridonate Gd(III) Complexes with Increased Hydration Number, Fast Water Exchange, Slow Electronic Relaxation, and High Relaxivity1. *J. Am. Chem. Soc.* 2007; 129(7):1870–1871. [PubMed: 17260995]

13. Aime S, Calabi L, Cavallotti C, Gianolio E, Giovenzana GB, Losi P, Maiocchi A, Palmisano G, Sisti M. [Gd-AAZTA]<sup>-</sup>: A New Structural Entry for an Improved Generation of MRI Contrast Agents. *Inorg. Chem.* 2004; 43(24):7588–7590. [PubMed: 15554621]
14. Xu J, Franklin SJ, Whisenhunt DW, Raymond KN. Gadolinium complex of tris[(3-hydroxy-1-methyl-2-oxo-1,2-didehydropyridine-4-carboxamido)ethyl]-amine: A New Class of gadolinium magnetic resonance relaxation agents. *J. Am. Chem. Soc.* 1995; 117(27):7245–7246.
15. Avedano S, Tei L, Lombardi A, Giovenzana GB, Aime S, Longo D, Botta M. Maximizing the relaxivity of HSA-bound gadolinium complexes by simultaneous optimization of rotation and water exchange. *Chem. Commun.* 2007; 45:4726–4728.
16. Aime S, Barge A, Borel A, Botta M, Chemerisov S, Merbach AE, Muller U, Pubanz D. A Multinuclear NMR Study on the Structure and Dynamics of Lanthanide(III) Complexes of the Poly(amino carboxylate) EGTA4- in Aqueous Solution. *Inorg. Chem.* 1997; 36(22):5104–5112.
17. Tei L, Baranyai Z, Botta M, Piscopo L, Aime S, Giovenzana GB. Synthesis and solution thermodynamic study of rigidified and functionalised EGTA derivatives. *Org. Biomol. Chem.* 2008; 6(13):2361–2368. [PubMed: 18563270]
18. Tei L, Botta M, Lovazzano C, Barge A, Milone L, Aime S. <sup>1</sup>H and <sup>17</sup>O NMR relaxometric study in aqueous solution of Gd(III) complexes of EGTA-like derivatives bearing methylenephosphonic groups. *Magn. Reson. Chem.* 2008; 46(Suppl 1):S86–S93. [PubMed: 18855344]
19. Senapati L, Schrier J, Whaley KB. Electronic Transport, Structure, and Energetics of Endohedral Gd@C82 Metallofullerenes. *Nano Lett.* 2004; 4(11):2073–2078.
20. Kato H, Suenaga K, Mikawa M, Okumura M, Miwa N, Yashiro A, Fujimura H, Mizuno A, Nishida Y, Kobayashi K, Shinohara H. Syntheses and EELS characterization of water-soluble multi-hydroxyl Gd@C82 fullereneols. *Chem. Phys. Lett.* 2000; 324(4):255–259.
21. Mikawa M, Kato H, Okumura M, Narazaki M, Kanazawa Y, Miwa N, Shinohara H. Paramagnetic Water-Soluble Metallofullerenes Having the Highest Relaxivity for MRI Contrast Agents. *Bioconjug. Chem.* 2001; 12(4):510–514. [PubMed: 11459454]
22. Funasaka H, Sakurai K, Oda Y, Yamamoto K, Takahashi T. Magnetic properties of Gd@C82 metallofullerene. *Chem. Phys. Lett.* 1995; 232(3):273–277.
23. Sitharaman B, Tran LA, Pham QP, Bolskar RD, Muthupillai R, Flamm SD, Mikos AG, Wilson LJ. Gadofullerenes as nanoscale magnetic labels for cellular MRI. *Contrast Media Mol. Imaging.* 2007; 2(3):139–146. [PubMed: 17583898]
24. Fillmore HL, Shultz MD, Henderson SC, Cooper P, Broaddus WC, Chen ZJ, Shu CY, Zhang J, Ge J, Dorn HC, Corwin F, Hirsch JI, Wilson J, Fatouros PP. Conjugation of functionalized gadolinium metallofullerenes with IL-13 peptides for targeting and imaging glial tumors. *Nanomedicine (Lond).* 2011; 6(3):449–458. [PubMed: 21542684]
25. Baxter AB, Lazarus SC, Brasch RC. In vitro histamine release induced by magnetic resonance imaging and iodinated contrast media. *Invest. Radiol.* 1993; 28(4):308–312. [PubMed: 7683008]
26. Bogdanov AA Jr, Weissleder R, Brady TJ. Long-circulating blood pool imaging agents. *Adv. Drug Delivery Rev.* 1995; 16:335–348.
27. Schuhmann-Giampieri G, Schmitt-Willich H, Frenzel T, Press W-R, Weinmann H-J. In Vivo and In Vitro Evaluation of Gd-DTPA-Polylysine as a Macromolecular Contrast Agent for Magnetic Resonance Imaging. *Invest. Radiol.* 1991; 26(11):969–974. [PubMed: 1743920]
28. Vexler VS, Clément O, Schmitt-Willich H, Brasch RC. Effect of varying the molecular weight of the MR contrast agent Gd-DTPA-polylysine on blood pharmacokinetics and enhancement patterns. *J. Magn. Reson. Imaging.* 1994; 4(3):381–388. [PubMed: 8061437]
29. Wen X, Jackson EF, Price RE, Kim EE, Wu Q, Wallace S, Charnsangavej C, Gelovani JG, Li C. Synthesis and Characterization of Poly(L-glutamic acid) Gadolinium Chelate: A New Biodegradable MRI Contrast Agent. *Bioconjug. Chem.* 2004; 15(6):1408–1415. [PubMed: 15546209]
30. Zhang G, Zhang R, Melancon MP, Wong K, You J, Huang Q, Bankson J, Liang D, Li C. The degradation and clearance of Poly(N-hydroxypropyl-L-glutamine)-DTPA-Gd as a blood pool MRI contrast agent. *Biomaterials.* 2012; 33(21):5376–5383. [PubMed: 22541356]

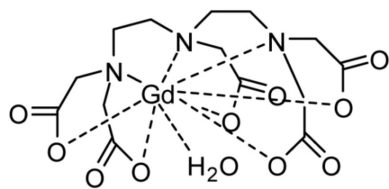
31. Berthezene Y, Vexler V, Kuwatsuru R, Rosenau W, Muhler A, Clement O, Price DC, Brasch RC. Differentiation of alveolitis and pulmonary fibrosis with a macromolecular MR imaging contrast agent. *Radiology*. 1992; 185(1):97–103. [PubMed: 1523341]
32. Yuan Z, Liu SY, Xiao XS, Zhong GR, Jiang QJ. Folate-poly-L-lysine-Gd-DTPA as MR contrast agent for tumor imaging via folate receptor-targeted delivery. *Zhonghua Yi Xue Za Zhi*. 2007; 87(10):673–678. [PubMed: 17553304]
33. Loubeyre P, Canet E, Zhao S, Benderbous S, Amiel M, Revel D. Carboxymethyl-dextran-gadolinium-DTPA as a blood-pool contrast agent for magnetic resonance angiography. Experimental study in rabbits. *Invest. Radiol*. 1996; 31(5):288–293. [PubMed: 8724128]
34. Sirlin CB, Vera DR, Corbeil JA, Caballero MB, Buxton RB, Mattrey RF. Gadolinium-DTPA-dextran: a macromolecular MR blood pool contrast agent. *Acad. Radiol*. 2004; 11(12):1361–1369. [PubMed: 15596374]
35. Åberg M, Hedner U, Bergentz S-E. THE ANTITHROMBOTIC EFFECT OF DEXTRAN. *Scand. J. Haematol*. 1979; 23(S34):61–68.
36. Wang SC, Wikstrom MG, White DL, Klaveness J, Holtz E, Rongved P, Moseley ME, Brasch RC. Evaluation of Gd-DTPA-labeled dextran as an intravascular MR contrast agent: imaging characteristics in normal rat tissues. *Radiology*. 1990; 175(2):483–488. [PubMed: 1691513]
37. Bumb A, Brechbiel MW, Choyke P. Macromolecular and dendrimer-based magnetic resonance contrast agents. *Acta Radiol*. 2010; 7:751–767. [PubMed: 20590365]
38. Mehvar R. Dextran for targeted and sustained delivery of therapeutic and imaging agents. *J. Control. Rel*. 2000; 69(1):1–25.
39. Helbich TH, Gossman A, Mareski PA, Raduchel B, Roberts TP, Shames DM, Muhler M, Turetschek K, Brasch RC. A new polysaccharide macromolecular contrast agent for MR imaging: biodistribution and imaging characteristics. *J. Magn. Reson. Imaging*. 2000; 11(6):694–701. [PubMed: 10862070]
40. Huang Y, Zhang X, Zhang Q, Dai X, Wu J. Evaluation of diethylenetriaminepentaacetic acid-manganese(II) complexes modified by narrow molecular weight distribution of chitosan oligosaccharides as potential magnetic resonance imaging contrast agents. *Magn. Reson. Imaging*. 2011; 29(4):554–560. [PubMed: 21277723]
41. Lebduskova P, Kotek J, Hermann P, Vander Elst L, Muller RN, Lukes I, Peters JA. A gadolinium(III) complex of a carboxylic-phosphorus acid derivative of diethylenetriamine covalently bound to inulin, a potential macromolecular MRI contrast agent. *Bioconjug. Chem*. 2004; 15(4):881–889. [PubMed: 15264877]
42. Schwickert HC, Roberts TP, Muhler A, Stiskal M, Demsar F, Brasch RC. Angiographic properties of Gd-DTPA-24-cascade-polymer--a new macromolecular MR contrast agent. *Eur. J. Radiol*. 1995; 20(2):144–150. [PubMed: 7588870]
43. Unger EC, Shen D, Wu G, Stewart L, Matsunaga TO, Trouard TP. Gadolinium-containing copolymeric chelates--a new potential MR contrast agent. *MAGMA*. 1999; 8(3):154–162. [PubMed: 10504042]
44. Kaneshiro T, Ke T, Jeong E-K, Parker D, Lu Z-R. Gd-DTPA L-cystine bisamide copolymers as novel biodegradable macromolecular contrast agents for MR blood pool imaging. *Pharmaceut. Res*. 2006; 23(6):1285–1294.
45. Mohs AM, Wang X, Goodrich KC, Zong Y, Parker DL, Lu Z-R. PEG-g-poly(GdDTPA-co-l-cystine): A Biodegradable Macromolecular Blood Pool Contrast Agent for MR Imaging. *Bioconjug. Chem*. 2004; 15(6):1424–1430. [PubMed: 15546211]
46. Roberts HC, Saeed M, Roberts TPL, Mühler A, Shames DM, Mann JS, Stiskal M, Demsar F, Brasch RC. Comparison of albumin-(Gd-DTPA)<sub>30</sub> and Gd-DTPA-24-cascade-polymer for measurements of normal and abnormal microvascular permeability. *J. Magn. Reson. Imaging*. 1997; 7(2):331–338. [PubMed: 9090587]
47. Lu Z-R, Parker DL, Goodrich KC, Wang X, Dalle JG, Buswell HR. Extracellular biodegradable macromolecular gadolinium(III) complexes for MRI. *Magn. Reson. Med*. 2004; 51(1):27–34. [PubMed: 14705042]

48. Zong Y, Wang X, Goodrich KC, Mohs AM, Parker DL, Lu Z-R. Contrast-enhanced MRI with new biodegradable macromolecular Gd(III) complexes in tumor-bearing mice. *Magn. Reson. Med.* 2005; 53(4):835–842. [PubMed: 15799038]
49. Ke T, Feng Y, Guo J, Parker DL, Lu Z-R. Biodegradable cystamine spacer facilitates the clearance of Gd(III) chelates in poly(glutamic acid) Gd-DO3A conjugates for contrast-enhanced MR imaging. *Magn. Reson. Imaging.* 2006; 24(7):931–940. [PubMed: 16916710]
50. Lu Z-R, Mohs AM, Zong Y, Feng Y. Polydisulfide Gd(III) chelates as biodegradable macromolecular magnetic resonance imaging contrast agents. *Intl. J. Nanomed.* 2006; 1:31–40.
51. Mohs AM, Nguyen T, Jeong E-K, Feng Y, Emerson L, Zong Y, Parker DL, Lu Z-R. Modification of Gd-DTPA cystine copolymers with PEG-1000 optimizes pharmacokinetics and tissue retention for magnetic resonance angiography. *Magn. Reson. Med.* 2007; 58(1):110–118. [PubMed: 17659618]
52. Tomalia DA, Naylor AM, Goddard WA. Starburst Dendrimers: Molecular-Level Control of Size, Shape, Surface Chemistry, Topology, and Flexibility from Atoms to Macroscopic Matter. *Angew. Chem. Int. Ed.* 1990; 29(2):138–175.
53. Bryant LH Jr, Brechbiel MW, Wu C, Bulte JW, Herynek V, Frank JA. Synthesis and relaxometry of high-generation (G = 5, 7, 9, and 10) PAMAM dendrimer-DOTA-gadolinium chelates. *J. Magn. Reson. Imaging.* 1999; 9(2):348–352. [PubMed: 10077036]
54. Nwe K, Xu H, Regino CAS, Bernardo M, Ileva L, Riffle L, Wong KJ, Brechbiel MW. A New Approach in the Preparation of Dendrimer-Based Bifunctional Diethylenetriaminepentaacetic Acid MR Contrast Agent Derivatives. *Bioconj. Chem.* 2009; 20(7):1412–1418. [PubMed: 19555072]
55. Nwe K, Bernardo M, Regino CAS, Williams M, Brechbiel MW. Comparison of MRI properties between derivatized DTPA and DOTA gadolinium-dendrimer conjugates. *Bioorg. Med. Chem.* 2010; 18(16):5925–5931. [PubMed: 20663676]
56. Konda SD, Aref M, Wang S, Brechbiel M, Wiener EC. Specific targeting of folate-dendrimer MRI contrast agents to the high affinity folate receptor expressed in ovarian tumor xenografts. *MAGMA.* 2001; 12(2–3):104–113. [PubMed: 11390265]
57. Swanson SD, Kukowska-Latallo JF, Patri AK, Chen C, Ge S, Cao Z, Kotlyar A, East AT, Baker JR. Targeted gadolinium-loaded dendrimer nanoparticles for tumor-specific magnetic resonance contrast enhancement. *Intl. J. Nanomed.* 2008; 3(2):201–210.
58. Cheng Z, Thorek DLJ, Tsourkas A. Gadolinium-Conjugated Dendrimer Nanoclusters as a Tumor-Targeted T1 Magnetic Resonance Imaging Contrast Agent. *Angew. Chem. Int. Ed.* 2010; 49(2): 346–350.
59. Huang C-H, Nwe K, Al-Zaki A, Brechbiel M, Tsourkas A. Biodegradable polydisulfide dendrimer nanoclusters as MRI contrast agents. *ACS Nano.* 2012 Articles ASAP.
60. Tilcock C, Unger E, Cullis P, MacDougall P. Liposomal Gd-DTPA: preparation and characterization of relaxivity. *Radiology.* 1989; 171(1):77–80. [PubMed: 2928549]
61. Fossheim SL, Fahlvik AK, Klaveness J, Muller RN. Paramagnetic liposomes as MRI contrast agents: influence of liposomal physicochemical properties on the in vitro relaxivity. *Magn. reson. imaging.* 1999; 17(1):83–89. [PubMed: 9888401]
62. Tilcock C, MacDougall P, Unger E, Cardenas D, Fajardo L. The effect of lipid composition on the relaxivity of Gd-DTPA entrapped in lipid vesicles of defined size. *Biochim. Biophys. Acta.* 1990; 1022(2):181–186. [PubMed: 2306454]
63. Kabalka GW, Buonocore E, Hubner K, Davis M, Huang L. Gadolinium-labeled liposomes containing paramagnetic amphipathic agents - targeted MRI contrast agents for the liver. *Magn. Reson. Med.* 1988; 8(1):89–95. [PubMed: 3173073]
64. Mody VV, Nounou MI, Bikram M. Novel nanomedicine-based MRI contrast agents for gynecological malignancies. *Adv. Drug Delivery Rev.* 2009; 61(10):795–807.
65. Discher BM, Won YY, Ege DS, Lee JCM, Bates FS, Discher DE, Hammer DA. Polymersomes: Tough vesicles made from diblock copolymers. *Science.* 1999; 284(5417):1143–1146. [PubMed: 10325219]
66. Katz JS, Zhong S, Ricart BG, Pochan DJ, Hammer DA, Burdick JA. Modular Synthesis of Biodegradable Diblock Copolymers for Designing Functional Polymersomes. *J. Am. Chem. Soc.* 2010; 132(11):3654–3655. [PubMed: 20184323]

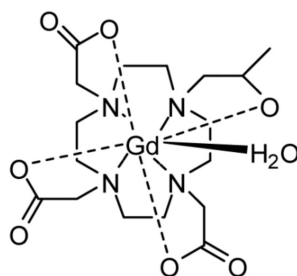


67. Cheng Z, Thorek DLJ, Tsourkas A. Porous Polymersomes with Encapsulated Gd-Labeled Dendrimers as Highly Efficient MRI Contrast Agents. *Adv. Funct. Mater.* 2009; 19(23):3753–3759. [PubMed: 23293575]
68. Cheng Z, Tsourkas A. Paramagnetic Porous Polymersomes. *Langmuir.* 2008; 24(15):8169–8173. [PubMed: 18570445]
69. Photos PJ, Bacakova L, Discher B, Bates FS, Discher DE. Polymer vesicles in vivo: correlations with PEG molecular weight. *J. Control. Rel.* 2003; 90(3):323–334.
70. Glogard C, Hovland R, Fossheim SL, Aasen AJ, Klaveness J. Synthesis and physicochemical characterisation of new amphiphilic gadolinium DO3A complexes as contrast agents for MRI. *J. Chem. Soc., Perkin Trans. 2.* 2000; (5):1047–1052.
71. Torres S, Martins JA, André JP, Geraldés CFGC, Merbach AE, Tóth É. Supramolecular Assembly of an Amphiphilic GdIII Chelate: Tuning the Reorientational Correlation Time and the Water Exchange Rate. *Chem. Eur. J.* 2006; 12(3):940–948. [PubMed: 16224764]
72. Tei L, Gugliotta G, Baranyai Z, Botta M. A new bifunctional GdIII complex of enhanced efficacy for MR-molecular imaging applications. *Dalton Trans.* 2009; 44:9712–9714. [PubMed: 19885512]
73. Kielar F, Tei L, Terreno E, Botta M. Large Relaxivity Enhancement of Paramagnetic Lipid Nanoparticles by Restricting the Local Motions of the GdIII Chelates. *J. Am. Chem. Soc.* 2010; 132(23):7836–7837. [PubMed: 20481537]
74. Turner JL, Pan D, Plummer R, Chen Z, Whittaker AK, Wooley KL. Synthesis of gadolinium-labeled shell-crosslinked nanoparticles for magnetic resonance imaging applications. *Adv. Funct. Mater.* 2005; 15:1248–1254.
75. Flacke S, Fischer S, Scott MJ, Fuhrhop RJ, Allen JS, McLean M, Winter P, Sicard GA, Gaffney PJ, Wickline SA, Lanza GM. Novel MRI Contrast Agent for Molecular Imaging of Fibrin. *Circulation.* 2001; 104(11):1280–1285. [PubMed: 11551880]
76. Lanza GM, Lorenz CH, Fischer SE, Scott MJ, Cacheris WP, Kaufmann RJ, Gaffney PJ, Wickline SA. Enhanced detection of thrombi with a novel fibrin-targeted magnetic resonance imaging agent. *Acad. Radiol.* 1998; 5 Supplement 1(0):S173–S176. [PubMed: 9561074]
77. Winter PM, Caruthers SD, Yu X, Song S-K, Chen J, Miller B, Bulte JWM, Robertson JD, Gaffney PJ, Wickline SA, Lanza GM. Improved molecular imaging contrast agent for detection of human thrombus. *Magn. Reson. Med.* 2003; 50(2):411–416. [PubMed: 12876719]
78. Winter P, Athey P, Kiefer G, Gulyas G, Frank K, Fuhrhop R, Robertson D, Wickline S, Lanza G. Improved paramagnetic chelate for molecular imaging with MRI. *J. Magn. Magn. Mater.* 2005; 293(1):540–545.
79. Lanza G, Winter P, Caruthers S, Hughes M, Hu G, Schmieder A, Wickline S. Theragnostics for tumor and plaque angiogenesis with perfluorocarbon nanoemulsions. *Angiogenesis.* 2010; 13(2):189–202. [PubMed: 20411320]
80. Cyrus T, Abendschein DR, Caruthers SD, Harris TD, Glattauer V, Werkmeister JA, Ramshaw JA, Wickline SA, Lanza GM. MR three-dimensional molecular imaging of intramural biomarkers with targeted nanoparticles. *J. Cardiovasc. Magn. Reson.* 2006; 8(3):535–541. [PubMed: 16755843]
81. Schmieder AH, Winter PM, Caruthers SD, Harris TD, Williams TA, Allen JS, Lacy EK, Zhang H, Scott MJ, Hu G, Robertson JD, Wickline SA, Lanza GM. Molecular MR imaging of melanoma angiogenesis with alphanubeta3-targeted paramagnetic nanoparticles. *Magn. Reson. Med.* 2005; 53(3):621–627. [PubMed: 15723405]
82. Taylor KML, Kim JS, Rieter WJ, An H, Lin W, Lin W. Mesoporous Silica Nanospheres as Highly Efficient MRI Contrast Agents. *J. Am. Chem. Soc.* 2008; 130(7):2154–2155. [PubMed: 18217764]
83. Kim J, Kim HS, Lee N, Kim T, Kim H, Yu T, Song IC, Moon WK, Hyeon T. Multifunctional Uniform Nanoparticles Composed of a Magnetite Nanocrystal Core and a Mesoporous Silica Shell for Magnetic Resonance and Fluorescence Imaging and for Drug Delivery. *Angew. Chem. Int. Ed.* 2008; 47(44):8438–8441.
84. Carniato F, Tei L, Dastru W, Marchese L, Botta M. Relaxivity modulation in Gd-functionalised mesoporous silicas. *Chem. Commun.* 2009; 10:1246–1248.

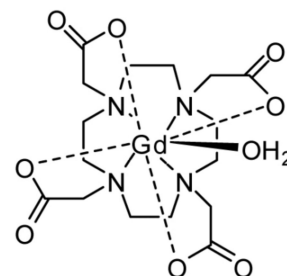
85. McDonald MA, Watkin KL. Investigations into the Physicochemical Properties of Dextran Small Particulate Gadolinium Oxide Nanoparticles. *Acad. Radiol.* 2006; 13(4):421–427. [PubMed: 16554221]
86. Engström M, Klasson A, Pedersen H, Vahlberg C, Käll P-O, Uvdal K. High proton relaxivity for gadolinium oxide nanoparticles. *Magn. Reson. Mater. Phys.* 2006; 19(4):180–186.
87. Fortin M-A, RM P Jr, Söderlind F, Klasson A, Engström M, Veres T, Käll P-O, Uvdal K. Polyethylene glycol-covered ultra-small Gd<sub>2</sub>O<sub>3</sub> nanoparticles for positive contrast at 1.5 T magnetic resonance clinical scanning. *Nanotechnology.* 2007; 18:395501.
88. Ahren M, Selegard L, Klasson A, Soderlind F, Abrikossova N, Skoglund C, Bengtsson T, Engstrom M, Kall PO, Uvdal K. Synthesis and characterization of PEGylated Gd<sub>2</sub>O<sub>3</sub> nanoparticles for MRI contrast enhancement. *Langmuir.* 2010; 26(8):5753–5762. [PubMed: 20334417]
89. Gu Z, Peng H, Hauge RH, Smalley RE, Margrave JL. Cutting Single-Wall Carbon Nanotubes through Fluorination. *Nano Lett.* 2002; 2(9):1009–1013.
90. Sitharaman B, Kissell KR, Hartman KB, Tran LA, Baikalov A, Rusakova I, Sun Y, Khant HA, Ludtke SJ, Chiu W, Laus S, Toth E, Helm L, Merbach AE, Wilson LJ. Superparamagnetic gadonanotubes are high-performance MRI contrast agents. *Chem. Commun.* 2005; 31:3915–3917.
91. Hartman KB, Laus S, Bolskar RD, Muthupillai R, Helm L, Toth E, Merbach AE, Wilson LJ. Gadonanotubes as ultrasensitive pH-smart probes for magnetic resonance imaging. *Nano Lett.* 2008; 8(2):415–419. [PubMed: 18215084]
92. Mackeyev Y, Hartman KB, Ananta JS, Lee AV, Wilson LJ. Catalytic Synthesis of Amino Acid and Peptide Derivatized Gadonanotubes. *J. Am. Chem. Soc.* 2009; 131(24):8342–8343. [PubMed: 19492838]
93. Raja KS, Wang Q, Gonzalez MJ, Manchester M, Johnson JE, Finn MG. Hybrid Virus-Polymer Materials. 1. Synthesis and Properties of PEG-Decorated Cowpea Mosaic Virus. *Biomacromolecules.* 2003; 4(3):472–476. [PubMed: 12741758]
94. Wang Q, Lin T, Tang L, Johnson JE, Finn MG. Icosahedral Virus Particles as Addressable Nanoscale Building Blocks. *Angew. Chem. Int. Ed.* 2002; 41(3):459–462.
95. Liepold LO, Abedin MJ, Buckhouse ED, Frank JA, Young MJ, Douglas T. Supramolecular protein cage composite MR contrast agents with extremely efficient relaxivity properties. *Nano Lett.* 2009; 9(12):4520–4526. [PubMed: 19888720]
96. Pokorski JK, Breitenkamp K, Liepold LO, Qazi S, Finn MG. Functional virus-based polymer-protein nanoparticles by atom transfer radical polymerization. *J. Am. Chem. Soc.* 2011; 133(24):9242–9245. [PubMed: 21627118]
97. AE, vdV. Reverse cholesterol transport: from classical view to new insights. *World J. Gastroenterol.* 2010; 16(47):5908–5915. [PubMed: 21157966]
98. Firestone RA. Low-Density Lipoprotein as a Vehicle for Targeting Antitumor Compounds to Cancer Cells. *Bioconjug. Chem.* 1994; 5(2):105–113. [PubMed: 8031872]
99. Corbin IR, Li H, Chen J, Lund-Katz S, Zhou R, Glickson JD, Zheng G. Low-density lipoprotein nanoparticles as magnetic resonance imaging contrast agents. *Neoplasia.* 2006; 8(6):488–498. [PubMed: 16820095]



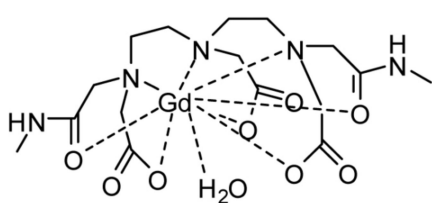
Magnevist (DTPA)  
( $r_1 = 3.8 \text{ mM}^{-1}\text{s}^{-1}$ )



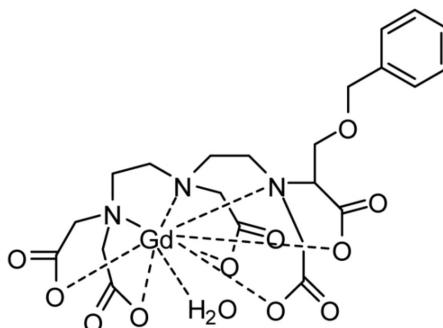
DO3A  
( $r_1 = 3.7 \text{ mM}^{-1}\text{s}^{-1}$ )



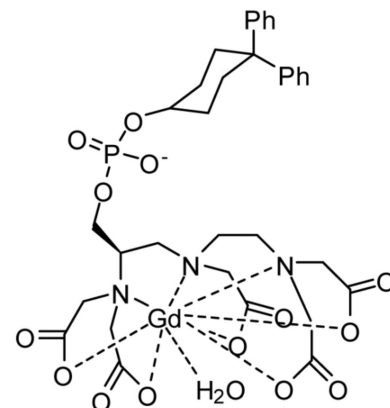
Dotarem (Gd-DOTA)  
( $r_1 = 3.5 \text{ mM}^{-1}\text{s}^{-1}$ )



Omniscan (Gd-DTPA-BMA)  
( $r_1 = 3.8 \text{ mM}^{-1}\text{s}^{-1}$ )

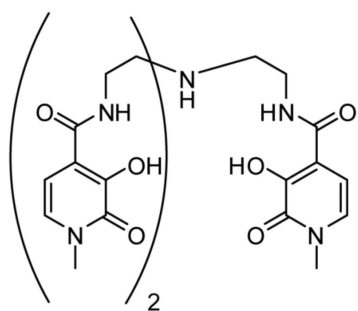


Multihance (Gd-BOPTA)  
( $r_1 = 4.8 \text{ mM}^{-1}\text{s}^{-1}$ )

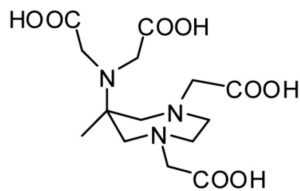


Vasovist (MS-325)  
( $r_1 = 6.8 \text{ mM}^{-1}\text{s}^{-1}$ )

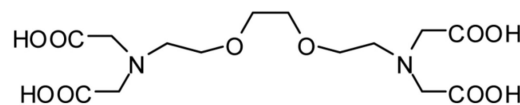
**Figure 1.**  
Clinically-approved and clinically-tested Gd-based contrast agents. All relaxivity values were acquired at 20 MHz, 310K.



TREN-1-Me-3,2-HOPO  
( $r_1 = 10.5 \text{ mM}^{-1}\text{s}^{-1}$ )

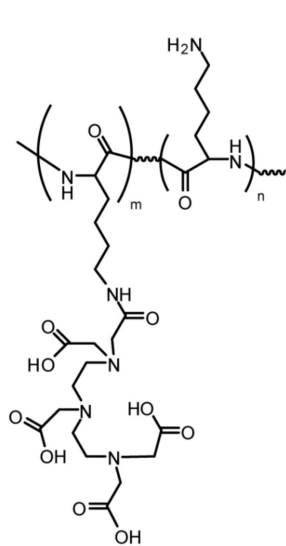


AAZTA  
( $r_1 = 14.0 \text{ mM}^{-1}\text{s}^{-1}$ )

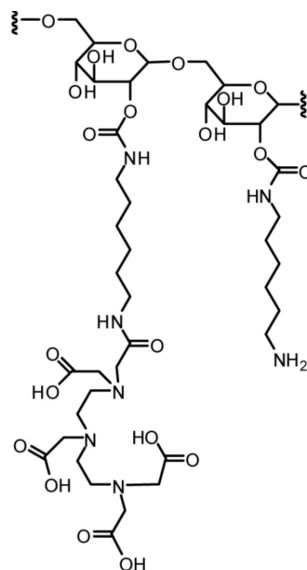


EGTA  
( $r_1 = 4.7 \text{ mM}^{-1}\text{s}^{-1}$ )

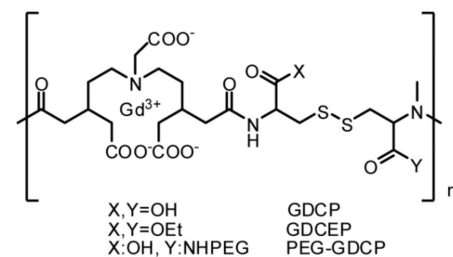
**Figure 2.**  
Examples of Gd ligands that exhibit improved  $r_1$  relaxivity, compared with current clinically-approved agents. All relaxivity values were acquired at 20 MHz, 298K.



DTPA-poly(L-lysine)



DTPA-labeled Dextran



Gd-DTPA Cystine Copolymer

**Figure 3.**  
Examples of Gd-labeled macromolecules that have been developed as contrast agents for magnetic resonance imaging.



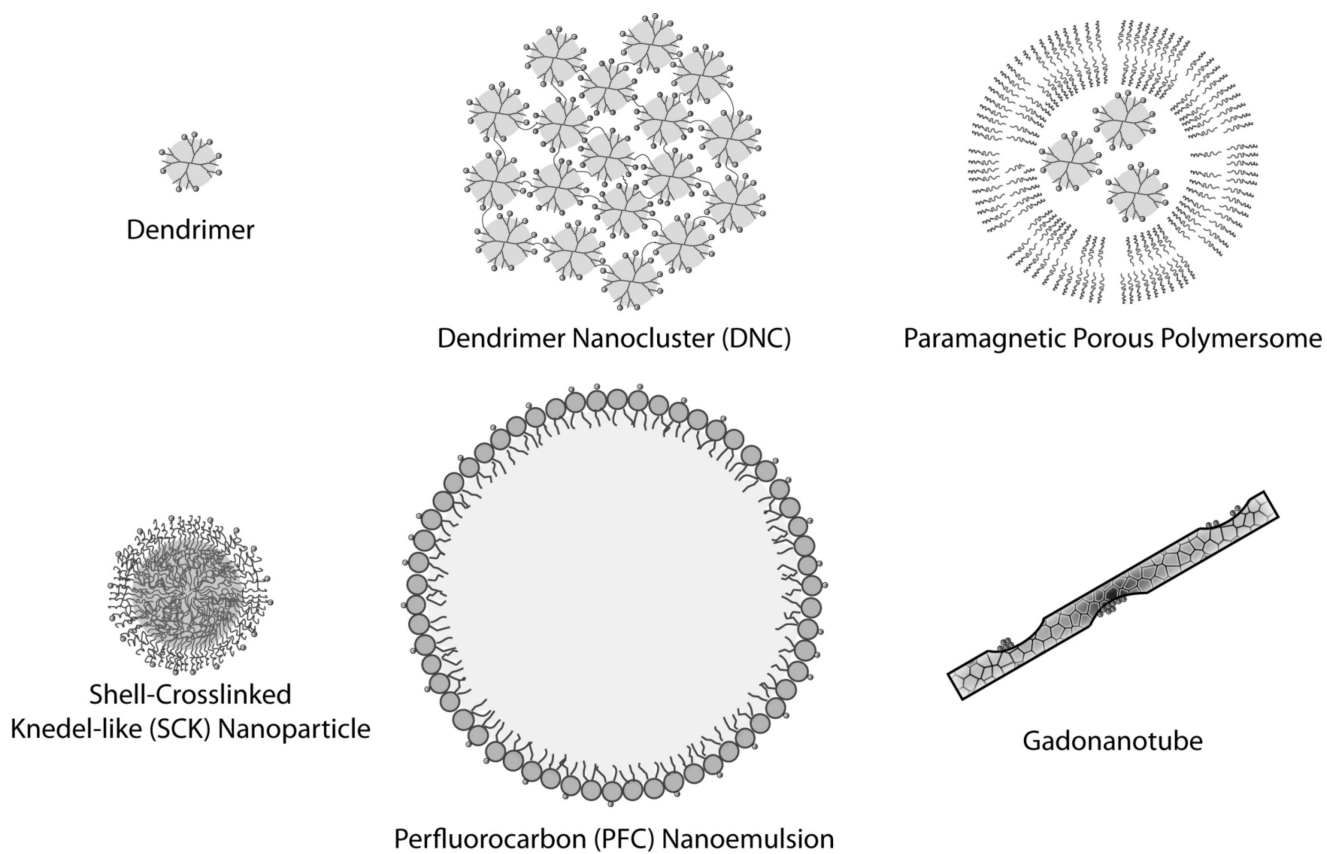


**Figure 4.** Examples of Gd-based nanoparticles that have been developed as contrast agents for magnetic resonance imaging.

**Table 1**  
Physical and magnetic properties of selected Gd-based nanoparticles and macromolecules

Nanoparticle	Hydrodynamic diameter (nm)/MW (kDa)	#Gd/particle	$r_1$ /Gd ( $\text{mM}^{-1}\text{s}^{-1}$ )	$r_1$ /particle ( $\text{mM}^{-1}\text{s}^{-1}$ )	Relaxivity density	ref.
Poly(L-lysine)-gadotetate dimeglumine	480 kDa	40	10.8 (0.4T, 39 °C)	432	0.9 ( $\text{mM}^{-1}\text{s}^{-1}/\text{kDa}$ )	[31]
Gd-DTPA-dextran	75 kDa	187	10.5 (0.25T, 37°C)	1,964	26.2 ( $\text{mM}^{-1}\text{s}^{-1}/\text{kDa}$ )	[36]
Cascade-Gd-DTPA-24	30 kDa	24	10 (2T, 37 °C)	240	8 ( $\text{mM}^{-1}\text{s}^{-1}/\text{kDa}$ )	[42, 46]
Gd-polydisulfide copolymer (cystine) GDGP	22 kDa	35	6.8 (3.0T)	238	10.8 ( $\text{mM}^{-1}\text{s}^{-1}/\text{kDa}$ )	[47-51]
G5-PAMAM dendrimer	5.4 nm/118 kDa	96	30 (20 MHz, 23°C)	2,880	34.9 ( $\text{mM}^{-1}\text{s}^{-1}/\text{nm}^3$ ) 24.4 ( $\text{mM}^{-1}\text{s}^{-1}/\text{kDa}$ )	[53]
G10-PAMAM dendrimer	13.5 nm/3000 kDa	1860	36 (20 MHz, 23°C)	66,960	51.8 ( $\text{mM}^{-1}\text{s}^{-1}/\text{nm}^3$ ) 22.3 ( $\text{mM}^{-1}\text{s}^{-1}/\text{kDa}$ )	[53]
Dendrimer nanocluster (DNC)	150 nm	300,000	12.3 (1.41T, 40°C)	3,600,000	2.0 ( $\text{mM}^{-1}\text{s}^{-1}/\text{nm}^3$ )	[58, 59]
Paramagnetic porous polymersome	130 nm	40,000	7.5 (1.41T, 40°C)	300,000	0.26 ( $\text{mM}^{-1}\text{s}^{-1}/\text{nm}^3$ )	[67, 68]
Micelle (shell-crosslinked knedel-like (SCK) nanoparticle	40±3 nm	513	39 (0.47T, 40°C)	20,000	0.6 ( $\text{mM}^{-1}\text{s}^{-1}/\text{nm}^3$ )	[74]
Perfluorocarbon (PFC) emulsion Gd-MeO-DOTA-PE	190 nm	49,329	29.8 (0.47T, 40°C)	1,470,000	0.4 ( $\text{mM}^{-1}\text{s}^{-1}/\text{nm}^3$ )	[78]
PEG-US-Gd <sub>3</sub> O <sub>3</sub>	2.8±1.1 nm	200	9.4 (1.5T, 20°C)	1880	163.6 ( $\text{mM}^{-1}\text{s}^{-1}/\text{nm}^3$ )	[87]
Gadonano tube	20-80 nm	100	180 (1.5T, 37°C)	18000	0.21 ( $\text{mM}^{-1}\text{s}^{-1}/\text{nm}^3$ )	[91]
Virus-like particle (VLP) P22 <sub>S39C</sub> -x-AEMA-Gd	71±3 nm	9,100±800	22 (1.4T)	200,000	1.07 ( $\text{mM}^{-1}\text{s}^{-1}/\text{nm}^3$ )	[95, 96]
Low density lipoprotein (LDL) nanoparticle	26.3 nm	180	8.1±0.19 (60MHz,40°C)	1440	0.15 ( $\text{mM}^{-1}\text{s}^{-1}/\text{nm}^3$ )	[99]